Biodegradation **13:** 239–250, 2002.
© 2002 *Kluwer Academic Publishers. Printed in the Netherlands.*

Mathematical modeling of precipitation and dissolution reactions in microbiological systems

Bruce E. Rittmann[1,*], James E. Banaszak[2], Jeanne M. VanBriesen[3] & Donald T. Reed[4]
[1]*Department of Civil and Environmental Engineering, Northwestern University, 2145 N. Sheridan Road, Evanston, IL 60208-3109, USA;* [2]*Exponent Failure Analysis Assoc., Two North Riverside Plaza, Suite 1400, Chicago, IL 60606, USA;* [3]*Department of Civil and Environmental Engineering, Carnegie-Mellon University, Pittsburgh, PA 15213-3890, USA;* [4]*24700 W. Easy St., Plainfield, IL 60544, USA (* author for correspondence)*

Accepted 19 August 2002

Key words: biogeochemistry, calcium carbonate, citrate, dissolution, ferric hydroxide, modeling, precipitation

Abstract

We expand the biogeochemical model CCBATCH to include a precipitation/dissolution sub-model that contains kinetic and equilibrium options. This advancement extends CCBATCH's usefulness to situations in which microbial reactions cause or are affected by formation or dissolution of a solid phase. The kinetic option employs a rate expression that explicitly includes the intrinsic kinetics for reaction or mass-transport control, the difference from thermodynamic equilibrium, and the aqueous concentration of the rate-limiting metal or ligand. The equilibrium feature can be used alone, and it also serves as check that the kinetic rate never is too fast and "overshoots" equilibrium. The features of the expanded CCBATCH are illustrated by an example in which the precipitation of $Fe(OH)_{3(s)}$ allows the biodegradation of citric acid, even though complexes are strong and not bioavailable. Precipitation releases citrate ligand, and biodegradation of the citrate increases the pH.

Introduction

The precipitation or dissolution of a solid phase can be an integral feature of biogeochemical systems whose chemistry is controlled by microbially catalyzed reactions. A selection of examples underscores the intimate interactions that can take place between solids and microbial reactions.

- Being colloids, microorganisms can serve as nucleation sites that increase the likelihood or rate of nucleation, the first step of precipitation.
- Microbial mineralization generates inorganic carbon that can increase the concentration of CO_3^{2-}, a common precipitating anion, such as with Ca^{2+} to form $CaCO_{3(s)}$.
- Precipitation typically removes bases – e.g., CO_3^{2-}, PO_4^{3-}, and OH^- – from solution, thereby decreasing the solution pH and possibly affecting microbial metabolism or viability.
- Precipitation of heavy metals can relieve inhibition of microbial metabolism.

The main goal of the research described here is to expand biogeochemical modeling so that it couples precipitation/dissolution reactions with the microbiological and aqueous geochemical reactions that inevitably occur at the same time. VanBriesen & Rittmann (1999) originally presented CCBATCH, a biogeochemical model that comprehensively couples the microbial reactions, which are kinetically controlled, to aqueous acid/base and complexation reactions, which are at equilibrium. This contribution builds upon VanBriesen & Rittmann (1999) by adding a sub-model for precipitation/dissolution, which can be kinetically controlled or at equilibrium. One of the challenges of this research is combining kinetic and equilibrium methods in such a manner that the correct approach is selected by the precipitation/dissolution sub-model, rather than requiring an *a priori* choice.

The presentation of how the sub-model is developed and implemented requires four parts. The first is a brief overview of CCBATCH, the biogeochemical model (VanBriesen & Rittmann 1999) that

is the foundation for the new precipitation/dissolution sub-model. The second is a critical review of the equilibrium and kinetic factors that control precipitation or dissolution and that must be reflected mathematically in the sub-model. The third is a description of the precipitation/dissolution sub-model; special emphasis is given to how kinetics and equilibrium are combined. The solid $CaCO_{3(s)}$ is used throughout parts two and three to make the general concepts tangible. The final part is an example that illustrates how the complete model can provide unique insights into a complex biogeochemical system in which precipitation and biodegradation interact. The example involves precipitation of $Fe(OH)_{3(s)}$, which releases citrate from its unavailable Fe^{3+} complex and accelerates citrate biodegradation.

The CCBATCH biogeochemical model

CCBATCH was designed at Northwestern University (VanBriesen & Rittmann 1999; Rittmann & VanBriesen 1996) to describe microbiological reactions in batch systems that have complex geochemical reactions. Aqueous-phase chemical reactions are acid/base and complexation, both of which reach thermodynamic equilibrium. They are modeled following well-known patterns of multi-component equilibria (e.g., Morel & Morgan 1972; Lichtner 1985, 1996). Chemical components can be combined through reactions to form every possible chemical species, but a component is unique and cannot be formed by a combination of other components. In CCBATCH, the components include all compounds formed or consumed by microbiological reactions: e.g., the cells ($C_5H_7O_2N$ by convention (Rittmann & McCarty 2001)), the electron-donor and -acceptor substrates, any intermediates, inorganic carbon (as H_2CO_3), and nitrogen (as NH_4^+).

Simultaneous solution of the coupled, non-linear mass balances for all components yields the equilibrium speciation. This is achieved by the SPECIATE sub-model, which uses a Newton-Raphson method (Press et al. 1992). CCBATCH can be run in a fixed-pH mode or with a variable pH predicted by the model. In the latter case, acid hydrogen is a component that is defined by the proton condition (VanBriesen & Rittmann 1999; Stumm & Morgan 1996), which is a mass balance on acid and base equivalents produced relative to reference levels established by the selection of the components.

Microbiological reactions are described in CCBATCH with a multiplicative-Monod formulation (Bae & Rittmann 1996):

$$r_{ut} = -q_{max}\frac{S}{K_s + S}\frac{A}{K_a + A}X \qquad (1)$$

where r_{ut} is the rate of substrate utilization ($M_sL^{-3}T^{-1}$), S is the concentration of the bioavailable form of the electron-donor substrate (M_sL^{-3}), A is the concentration of the electron-acceptor substrate (M_aL^{-3}), and X is the concentration of active biomass (M_xL^{-3}). Three parameters describe the kinetics of substrate utilization: q_{max}, the maximum specific rate of utilization of the electron-donor substrate by the cells ($M_sM_x^{-1}T^{-1}$); K_s, the donor concentration giving one-half the maximum rate (M_sL^{-3}); and K_a, the acceptor concentration giving one-half the maximum rate (M_aL^{-3}). The rate of substrate utilization determined by the multiplicative-Monod expression is then coupled with stoichiometry describing the utilization of donor and acceptor substrates to generate new biomass to compute the rates of change in mass for all components involved in the microbial reaction (VanBriesen & Rittmann 1999; Rittmann & VanBriesen 1996).

For each time step modeled, the rates of consumption or production of components are transferred to the master SOLVER sub-model, which updates total concentrations of all components. SOLVER then calls the SPECIATE sub-model, which respeciates all components subject to equilibrium for all acid/base or complexation reactions. These new concentrations are then used to compute rates for the next time step, in which the same procedure repeats.

Mechanisms of precipitation and dissolution

In many natural systems, the pH of water is buffered by the precipitation and dissolution of minerals, usually metal oxides, hydroxides, and carbonates (Stumm & Morgan 1996). Although many of these reactions are kinetically controlled, it is useful here to begin with the simple case of equilibrium between the solid and aqueous phases. Calcite, $CaCO_{3(s)}$, a common mineral, serves as a tangible example.

By convention, solid-phase reactions are written as dissolutions. For calcite at 25 C (Stumm & Morgan 1996):

$$CaCO_{3(s)} \Leftrightarrow Ca^{2+} + CO_3^{2-}$$

$$K_{sp} = 10^{-8.34} = \{Ca^{2+}\}\{CO_3^{2-}\} \quad (2)$$

where K_{sp} is defined as the solubility product and { } refers to thermodynamic activity. The expression for K_{sp} assumes that the activity of the solid phase equals 1. Once the activity of CO_3^{2-} is known, the equilibrium activity of is Ca^{2+} determined from Equation (2). Equation (2) also shows that precipitation of one mole of $CaCO_{3(s)}$ removes 1 mole of CO_3^{2-}, which is a base.

Modeling requires that mass concentrations be used to satisfy mass balances. Within CCBATCH, activities are converted to mole/l concentrations by using activity coefficients (γ) that depend on the solution's ionic strength (Stumm & Morgan 1996; VanBriesen & Rittmann 1999). Equation (2) can be rewritten in the concentration regime:

$$^{c}K_{sp} = \frac{K_{sp}}{\gamma_{Ca^{2+}}\gamma_{CO_3^{2-}}} = [Ca^{2+}][CO_3^{2-}] \quad (3)$$

where $^{c}K_{sp}$ is the concentration solubility product, [ ] refers to mole/l concentration, and $\gamma_{Ca^{2+}}$ and $\gamma_{CO_3^{2-}}$ refer to the activity coefficients for Ca^{2+} and CO_3^{2-}, respectively.

Although thermodynamic equilibrium is a good starting point, solid-phase precipitation and dissolution often are kinetically controlled reactions. Solid nucleation, crystal growth, and solid dissolution are distinctly different mechanisms that can control the kinetics.

Solid nucleation

As a homogeneous solution becomes super-saturated, i.e., $[Ca^{2+}][CO_3^{2-}] > {}^{c}K_{sp}$, the random reaction between the two solid precursors can form a "pure" particle of solid. However, very small particles have exceedingly high surface area to volume ratios, with correspondingly high interfacial areas that have surface energy (Flint 1963; Stumm & Morgan 1996). If the energy gain caused by solid formation is not sufficient to overcome the energy required to form the new surface, the particle will redissolve or not grow. However, if the particle formed is large enough, the release of energy from formation of new solid will overcome the energy cost of creating new surface area. This initiation of solid formation from pure liquid phases is known as *homogeneous nucleation*.

In most environmental systems, precipitates are formed in the presence of other solid particles, such as mineral and biological surfaces and suspended colloidal particles. In these systems, precipitation is preceded by *heterogeneous nucleation*, i.e., part of the nucleus surface is in contact with another solid, and part is in contact with the liquid phase (Stumm & Morgan 1996). When the forming nucleus is compatible with the present solid surface, the energy of nucleation is minimized, and nucleation is promoted (Flint 1963; Stumm & Morgan 1996). Heterogeneous nucleation seems to be preceded by surface complexation or polynuclear complex formation at kink sites on solid surfaces (Brady & House 1996; Lasaga 1995; Lasaga et al. 1994; Paquette & Reeder 1995). Microbial cell membranes can serve as nucleation sites; therefore, nucleation is unlikely to be a rate-controlling mechanism for situations in which CCBATCH is applied.

Crystal growth

Solid surfaces are not homogeneous structures, but consist of numerous defects, sites where the crystal structure is interrupted. Because these defect sites affect the lattice integrity of the adjacent crystals, they tend to serve as the active sites for the dissolution or precipitation of the solid (Brady & House 1996; Jordan & Rammensee 1996; Lasaga 1995; Lasaga et al. 1994; Morel & Hering 1993; Paquette & Reeder 1995; Stumm & Morgan 1996). The availability of reactive sites, which should be proportional to the surface area of the solid particle, directly affects the rate of crystal growth.

In addition to a dependence on surface area, solid crystal growth rates can be controlled by one or more of (1) the mass transfer of reacting species to the solid surface, (2) surface adsorption of one or more reacting species, (3) diffusion across the surface, (4) reaction at the solid surface active site, and (5) incorporation of the new precipitate into the crystal lattice (Brady & House 1996). Most often, (1) or (4) is the rate-controlling step in precipitation reactions (Brady & House 1996). Since mechanistically these two steps are different, the mathematical descriptions of the processes also may differ.

The overall rate of surface reaction is limited by step (4), *the rate of the chemical reaction*, when the solution concentrations of the reactive species are close to equilibrium with the solid. For example, calcite precipitation/dissolution can be considered microscopically reversible at high pH and low CO_2 partial pressure (Morel & Hering 1993). Following Morel

& Hering (1993), the dissolution rate r_d normalized to surface area is equal to a constant coefficient (k_d, $ML^{-2}T^{-1}$) near equilibrium:

$$r_d = k_d \tag{4}$$

The precipitation rate depends on the concentrations of the two reactive species:

$$r_p = k_p[Ca^{2+}][CO_3^{2-}] \tag{5}$$

where r_p is the surface-normalized precipitation rate ($ML^{-2}T^{-1}$) and k_p is the second-order precipitation rate coefficient ($L^4M^{-1}T^{-1}$)

Assuming that the calcite reaction is reversible,

$${}^cK_{sp} = [Ca^{2+}][CO_3^{2-}] = \frac{k_d}{k_p} \tag{6}$$

then, the net rate of precipitation is the difference between the precipitation and dissolution rates:

$$r_p^{net} = r_p - r_d = k_p[Ca^{2+}][CO_3^{2-}] - k_d. \tag{7}$$

Substituting $k_d = k_p\ {}^cK_{sp}$ (from Equation (6)) into Equation (7) and rearranging give

$$\begin{aligned} r_p^{net} &= k_p([Ca^{2+}][CO_3^{2-}] - {}^cK_{sp}) \\ &= k_p\ {}^cQ\left(\frac{{}^cK_{sp}}{{}^cQ}\right) \end{aligned} \tag{8}$$

where ^cQ equals the actual reaction product of the reacting species, or $^cQ = [Ca^{2+}][CO_3^{2-}]$.

Often precipitation/dissolution reactions depend on the concentration of only one of the reacting species, the other being relatively constant. Notable examples include calcite precipitation in an open system and metal-hydroxide precipitation at fixed pH. In this case, $[CO_3^{2-}]$ can be taken as a constant in the ^cQ term outside the brackets in Equation (8). Making this substitution and multiplying it by the specific surface area, a (L^{-1}), give

$$R_p^{net} = k'a\left(1 - \frac{{}^cK_{sp}}{{}^cQ}\right)[Ca^{2+}] \tag{9}$$

where $k' = k_p[CO_3^{2-}]$ and R_p^{net} is the net rate in concentration units ($ML^{-3}T^{-1}$) or $R_p^{net} = r_p^{net}a$.

It is necessary to compare Equation (9) to a rate equation derived from mass-transport limitation of precipitation, i.e., step (1) above. Once again, the rate of surface reaction often depends only on the concentration of the metal in solution, the ligand concentration either being in great excess or relatively constant. For the $CaCO_{3(s)}$ case, the rate of surface reaction is controlled by the disequilibrium between the metal concentration that would be in equilibrium with the solid surface ($[Ca^{2+}]_{eq}$) and the actual metal concentration $[Ca^{2+}]$:

$$R_p = ka([Ca^{2+}] - [Ca^{2+}]_{eq}) \tag{10}$$

or

$$R_p = ka\left(1 - \frac{[Ca^{2+}]_{eq}}{[Ca^{2+}]}\right)[Ca^{2+}] \tag{11}$$

where k is the mass-transport rate coefficient for Ca^{2+} (LT^{-1}). Since $[Ca^{2+}]_{eq} = {}^cK_{sp}/[CO_3^{2-}]$ and $[Ca^{2+}] = {}^cQ/[CO_3^{2-}]$, the rate expression reduces to:

$$R_p = ka\left(1 - \frac{{}^cK_{sp}}{{}^cQ}\right)[Ca^{2+}] \tag{12}$$

which has the same form as Equation (9). Even though the mechanistic bases for k and k′ differ, the rate expressions are of the same form whether surface reaction or mass transfer limits. In either case, when $^cQ > {}^cK_{sp}$, the solution is super-saturated, and $R_p > 0$, which corresponds to a net *gain* of solid and a net *loss* of Ca^{2+} from solution.

In modeling actual systems, it is often difficult to separate the rate coefficient, k or k′, from the solid surface area, a. However, when homogeneous nucleation is not relevant, often the surface area is relatively unaffected by the solid precipitation/dissolution. In these cases, k or k′ and a can be lumped together into one overall term, ka or k′a.

Solid dissolution

Under conditions near equilibrium, mineral dissolution rates can be treated as reversible reactions. In these cases, the rate law is the same as Equation (9) for the near-equilibrium precipitation of calcite (Morel & Hering 1993). Sometimes mineral dissolution occurs in dilute solutions far from equilibrium and can be promoted or inhibited by the presence of aqueous species that pull the speciation away from equilibrium. The simplest model of mineral dissolution far from equilibrium assumes that the dissolution rate (R_d, $ML^{-3}T^{-1}$) is limited by *mass transfer* of dissolved species away from the solid surface. When one species concentration is relatively constant, it is apparent that the rate

expression is the same as derived for mass-transfer-limited precipitation (Equation (12)), although with the opposite sign. Again, for $CaCO_{3(s)}$,

$$R_d = -R_p = -ka\left(1 - \frac{{}^cK_{sp}}{{}^cQ}\right)[Ca^{2+}]. \qquad (13)$$

When the Ca^{2+} concentration is very small,

$$\left(1 - \frac{{}^cK_{sp}}{{}^cQ}\right)$$

aproaches

$$\left(-\frac{{}^cK_{sp}}{{}^cQ}\right) = -\frac{{}^cK_{sp}}{[Ca^{2+}][CO_3^{2-}]},$$

and Equation (13) approaches the limit case of

$$R_d = \frac{ka\,{}^cK_{sp}}{[CO_3^{2-}]} \qquad (14)$$

Thus, in an under-saturated solution far from equilibrium with the solid phase, mass-transport-controlled dissolution reaches a maximum rate that is independent of the solution concentration of the metal cation (Brady & Zachara 1996; Morel & Hering 1993; Stumm & Morgan 1996), but is inversely proportional to the concentration of the anionic ligand.

Comparison of rate expression

Table 1 summarizes and generalizes the precipitation-rate equations. For generality, $[Ca^{2+}]$ is replaced by [Me], $[CO_3^{2-}]$ is replaced by [L], and ${}^cQ$ = [Me][L]. The dissolution rate simply takes the opposite sign. The key trend in Table 1 is that each mechanistic model yields an expression of the form:

$$R_p = k'a\left(1 - \frac{{}^cK_{sp}}{{}^cQ}\right)[Me]. \qquad (15)$$

We use this generalized kinetic form in the precipitation/dissolution sub-model of CCBATCH. This form contains three parts. The first k′a, is which is the lumped product of reaction or mass transfer rate times the specific surface area. The second part is $(1 - {}^cK_{sp}/{}^cQ)$, which expresses the thermodynamic state of the system through a "difference from equilibrium". When ${}^cK_{sp}/{}^cQ = 1$, the system is at equilibrium, and $({}^cK_{sp}/{}^cQ)$ equals zero, ensuring no net reaction. When ${}^cK_{sp}/{}^cQ < 1$, the system is super-saturated, and R_p is positive. The difference-from-equilibrium method requires that the solubility-limiting solid be identified and its K_{sp} estimated. Finally, the aqueous concentration of the rate-controlling metal [Me], which quantifies the rate expression in actual-mass units.

The new sub-model, described in detail in the next section, allows CCBATCH to describe precipitation/dissolution reactions that are caused by changes in aqueous-phase speciation. This capability is relevant for many common carbonate, hydroxide, sulfide, and phosphate solids (Stumm & Morgan 1996). Changes in aqueous-phase speciation often are brought about by microbially catalyzed redox reactions (VanBriesen & Rittmann 1999; Stumm & Morgan 1996), and the new sub-model has as its main goal to make this connection. On the other hand, the sub-model does not explicitly describe reductive dissolution reactions in which the microorganisms work directly on the solid surface (e.g., Myers & Myers 1993; Lovley 1991).

The precipitation/dissolution sub-model

The precipitation/dissolution sub-model added to CCBATCH contains kinetic and equilibrium features that can be selected by the user. If the user selects the equilibrium approach, the kinetic feature is disengaged. At each time step, the equilibrium feature ensures that the product of concentrations of the metal cation and ligand anion equal ${}^cK_{sp}$. If the user selects the kinetic approach, Equation (15) is used to compute a rate of precipitation or dissolution based on k′a, ${}^cK_{sp}$, ${}^cQ$, and [Me] for that time step. This rate is used to compute the changes in mass to any component involved in the precipitation/dissolution reaction. The SOLVER part of CCBATCH adjusts the masses of all aqueous components, as well as the mass of the solid phase, based on the rates returned from the precipitation/dissolution sub-model.

When the user selects the kinetic approach, the equilibrium feature is not disengaged. Instead, it is used in parallel to the kinetic feature in order to ensure that the kinetic computation never "overshoots," or goes from one side of equilibrium to the other side due solely to a precipitation or dissolution reaction. This equilibrium "check" is an essential and unique part of the sub-model and is described in detail later.

The SOLVER sub-model calls the precipitation/dissolution sub-model after equilibrium speciation and all microbiological reaction rates are deter-

Table 1. Comparison of the forms of the precipitation rate equations

Mechanistic model	Rate expression for precipitation, R_p	k'	Special conditions
Reversible equilibrium	$k'a\left(1 - \frac{^cK_{sp}}{^cQ}\right)$ [Me]	k_p [L]	[L] ≈ constant
Mass-transport controlled ppt/dss	$k'a\left(1 - \frac{^cK_{sp}}{^cQ}\right)$ [Me]	k	Rate dependent only on Me transport

mined. The precipitation/dissolution sub-model requires the following input information:

- The identity of the solid component.
- The stoichiometry of the solid-dissolution reaction.
- The solubility product (i.e., $^cK_{sp}$) for the solid-dissolution reaction.
- The identity of the rate-controlling species (i.e., [Me] in Equation (15)).
- The kinetic parameters describing the fixed surface area rate constant, $k'a$, for precipitation and dissolution.

The sub-model sets the activity of each solid phase to 1 (currently the model is based on the formation of pure solid phases) and calculates ^cQ, the ion-activity product of the solid reaction, based on the equilibrium speciation calculated previously for the given time step.

Once ^cQ is calculated, a checking routine is used to evaluate the state of the system. If ^cQ is greater than the equilibrium constant, the system is super-saturated, and a precipitation rate is calculated and sent to the SOLVER, which updates the component concentrations based on the kinetic (and concurrent biological) reaction rates (VanBriesen & Rittmann 1999). If ^cQ is less than the equilibrium constant, the system is under-saturated. The model then checks to determine if any solid is in the system. If no solid is present, no rate is calculated. If solid is present, a dissolution rate is calculated and sent to the SOLVER.

Equilibrium precipitation/dissolution

Inspection of the form of the precipitation rate equation (Equation (15)) shows that the rate calculated by this expression can range over many orders of magnitude. This effect is most pronounced when precipitation or dissolution is initiated in a greatly super- or under-saturated system, respectively. In these cases, the rate calculated in one time step can be very large. Our preliminary modeling work indicated that, in some cases, the rate calculated in a single time step was so large that the kinetic algorithm "overshot" the equilibrium condition. For example, a solution greatly super-saturated had such a large precipitation rate that the loss of component mass drove the reaction to under-saturated in one time step. To avoid this error, we developed a solid-equilibrium subroutine to set limits for the kinetic algorithm. In this way, the rate of precipitation/dissolution calculated by the kinetic algorithm is checked during each time step to avoid "overshooting" the equilibrium condition. This equilibrium feature also can be selected by a user who chooses not to describe precipitation/dissolution as kinetically controlled.

In geochemical modeling, two methods are used for calculating aqueous chemical equilibria with precipitating or dissolving solid phases (Bethke 1992; Morel & Morgan 1972). In a static system (i.e., a one-time equilibrium calculation) or in a system in which the solid is always present (does not dissolve completely), the simplest method for calculating solid equilibria is to write the component basis in terms of the solid phase. In this case, all the aqueous species are "complexes" of the component solid. In the equilibrium expressions for these "complexes," the activity of this component is the activity of a solid phase, almost always 1. This method works well for *strictly* equilibrium calculations, and it would work in CCBATCH, as long as the solid phase always were present.

The solid-component approach is inadequate when the solid phase completely dissolves or when precipitation must begin from a homogeneous, dynamic aqueous system. In the case of complete dissolution, if (mathematically) the component concentration goes to zero, so do the "complex" concentrations. However, we know from conservation of mass that, when all of a solid dissolves, its ions distribute among one or more aqueous species. Similarly, when a solid exists in a system at equilibrium, the relative concentrations of the ions that make up the solid are fixed by the solubility product. Simply stated, the

solid cannot be the component when it does not exist. Thus, upon complete dissolution of a solid (or, initiation of precipitation from a homogeneous liquid system), the component basis must be re-written in terms of one of the dissolved ions from the solid to account for this discontinuity correctly. This concept is called "basis switching" and is used successfully in several geochemical models capable of handling multiple solids (e.g., *The Geochemist's Workbench*, Bethke 1992). The major advantage of this method for calculating chemical equilibrium involving solid phases is computational efficiency.

In the alternate methodology, the component basis is fixed and written in terms of an ionic species, e.g., the fixed component for calcite is Ca^{2+}. This alternate method couples better to kinetic mass-transfer expressions. Using calcite precipitation in an under-saturated, open system (i.e., the carbonate concentration is independent of calcite precipitation) as an example, when chemical conditions in the system change, as long as calcite remains under-saturated, the mathematical description of the system is correct. As soon as calcite becomes over-saturated, mass (Ca^{2+} and CO_3^{2-}) must be transferred from the aqueous phase to the solid phase to re-attain equilibrium.

It is easy to conceptualize how to use this incremental kinetic calculation to determine the equilibrium condition. For a simple calcite system, we incrementally make the kinetic mass transfer coefficient larger until just the right amount of calcite is precipitated (in a given time step) and the exact amount of the component, Ca^{2+}, is removed, so that the saturation index (${}^{c}K_{sp}/{}^{c}Q$) for calcite equals one (Morel & Morgan 1972). As solid phases become super- or under-saturated with respect to the equilibrium aqueous speciation, mass is successively transferred into or out of the aqueous system until all of the solid dissolves or the remaining aqueous species are at equilibrium with the solid.

The rate calculated when the amount of mass transferred into or out of solution just attains equilibrium is significant to the CCBATCH application. It is the "maximum" rate (for a given time step) that mass can be transferred without overshooting the equilibrium point. By comparing the rate calculated by the actual kinetic expression (Equation (15)) to this maximum rate, we can ensure that model calculations in a dynamic system do not defy thermodynamics by overshooting equilibrium. The key to determining the maximum rate is calculating the correct adjustment to the component concentrations, for this example, Ca^{2+} and CO_3^{2-}, so that equilibrium is attained.

Because of its inherent benefits, we use the second approach for implementing equilibrium precipitation/dissolution into the sub-model. The major steps of this equilibrium feature are:

1. An initial guess for the total component concentration is made for the metal species associated with the solid. In the current code, this is a preset value, 1×10^{-15} M. The range of component concentrations allowed by the model currently is 10^{-30} to 1 M.
2. The difference between the guess concentration of the metal component and the initial value is computed. For example, for calcite dissolution when the initial Ca^{2+} concentration is 0, the first difference calculated is $1 \times 10^{-15} - 0 = 10^{-15}$ M.
3. The total concentrations of all components that participate in the solid reaction are adjusted using the difference calculated in step (2) and the dissolution-reaction stoichiometry. For this calcite example, the component concentration of CO_3^{2-} is increased by 10^{-15} M. The new total component values are sent to the aqueous-speciation model, which returns the chemical speciation of all the components and complexes in solution. So, in the first iteration for calcite dissolution, the speciation is calculated based on the total Ca^{2+} component concentration given in step 2 above, 1×10^{-15} M, and the adjusted total concentrations of the other components affected by calcite dissolution.
4. The reaction product, ${}^{c}Q$, is calculated based on the updated speciation to determine if the system is super- or under-saturated. Using the bisection method, the total component concentrations are adjusted again, and steps 2 to 4 are repeated. Continuing with the calcite example, when the Ca^{2+} component concentration is 10^{-15} M, the solution is still under-saturated with respect to calcite. A new guess concentration is calculated by bisecting the difference between the last guess, 10^{-15} M, and the maximum allowed concentration, 1M. The actual numerical calculations are based on the log of the concentration to improve numerical accuracy.
5. Steps 2 to 4 repeat until a specified convergence tolerance is met or if the preset maximum number of iterations is exceeded. In the former case, convergence is currently set to when the new guess concentration differs from the last guess by less

than 10^{-12} M, converted to log units. In the latter case, an error message is generated.

6. The solution returned to the SOLVER sub-model is the total component concentration of the metal component in the solid that is in equilibrium with the system for the initial conditions. For example, if calcite were under-saturated, the value for the total Ca^{2+} concentration returned from the subroutine would be higher than the initial concentration.
7. The SOLVER sub-model calculates the maximum precipitation (or dissolution) rate from the difference between the initial total component concentration and the value returned from the equilibrium subroutine.
8. The maximum precipitation (or dissolution) rate is compared to the rate computed based on kinetics. The smaller of the two rates is used to calculate the amount of mass transferred to or from the solid in the current time step.

Incorporation into CCBATCH and testing

Consistent with the rest of CCBATCH (VanBriesen & Rittmann 1999), the precipitation/dissolution sub-model was coded in FORTRAN and uses double-precision variables. The complete FORTRAN code for the sub-model is listed in Banaszak (1999). Implemented into CCBATCH, the sub-model retrieves all information it needs from SOLVER. Information passed between the precipitation/dissolution sub-model and the SOLVER sub-model includes the total component concentrations, the dissolution reaction stoichiometry (recall that solid-phase reactions must be written as dissolution reactions), and the solubility product for the solid dissolution reaction. The equilibrium-solution algorithm is based on the bisection method adapted from Borse (1991).

We performed extensive testing to ensure that the implemented sub-model achieves mass-balance closure, proceeds to an exact equilibrium solution, and perfectly reproduces the results for special cases for which analytical solutions are available (Banaszak 1999).

Example: the iron (III)-citrate-P. fluorescens system

Citric acid ($C_6H_5O_7H_3$), abbreviated H_3Cit, is a key intermediate in the tricarboxylic acid (TCA) cycle, and many respiring organisms can use it as an energy and carbon source (Madigan et al. 2000). VanBriesen & Rittmann (1999) used citric acid to illustrate how the basic CCBATCH works and how speciation among the many acid/base and complex forms of citrate controls its biodegradation rate. In particular, VanBriesen & Rittmann (1999) predicted the effects of pH and Fe^{3+} complexation on the rate and extent of citrate biodegradation when $HCit^{2-}$ (the twice-dissociated form of citric acid) is the bioavailable species. This means that the $HCit^{2-}$ concentration is used as S in the Monod expression (Equation (1)). Increasing pH from 6 to 8 nearly stops biodegradation, since the acid/base speciation is shifted from $HCit^{2-}$ to Cit^{3-} ($p^cK_{a,3}$ for $HCit^{2-} \leftrightarrow H^+ + Cit^{3-}$ is 5.8 for an ionic strength of 0.1). Thus, the concentration of the bioavailable rate controlling $HCit^{2-}$ is very small, making the utilization rate small. Addition of Fe^{3+} to solution essentially stops citrate biodegradation whenever the Fe^{3+}: Citrate mole ratio is greater than or equal to one, because Fe^{3+} forms strong citrate complexes that sequester citrate away from the bioavailable $HCit^{2-}$ form.

Joshi-Topé & Francis (1995) performed experiments with a system containing Fe^{3+}, citrate, and *Pseudomonas fluorescens*. In their experiments, dissolved oxygen was amply available and not limiting, and the pH was not buffered. The data points in Figure 1 are from experiments without Fe^{3+} added (left panel) or with Fe^{3+} added in a 1 : 1 mole ratio (right panel). Although the rate of citric-acid degradation was slower when Fe^{3+} was added, citrate was significantly biodegraded over 50h in the batch experiment with Fe^{3+} added. Fe^{3+} was not measured. We use CCBATCH with the precipitation/dissolution sub-model to explore how precipitation of $Fe(OH)_{3(s)}$ explains the observation of citrate biodegradation despite additions of Fe^{3+} at a 1 : 1 mole ratio with citrate.

Hamm et al. (1954) studied the complexation of Fe in citrate solutions. In Fe (III) systems, Hamm et al. (1954) postulated that three complexes are formed between Fe and citrate: $FeCit^0$, $Fe(OH)Cit^-$, and $Fe(OH)_2Cit^{2-}$. The formation constants for these species, along with constants for other complexes considered in this modeling, are shown in Table 2. At pH 6.0 to 6.1, the initial pH used in the experiments (Joshi-Topé & Francis 1995), equilibrium calculations show that the $Fe(OH)Cit^-$ complex accounts for about 97% of the Fe and citric acid in solution. As the pH of the system increases due to biodegradation of citrate (VanBriesen & Rittmann 1999), the $Fe(OH)_2Cit^{2-}$ complex becomes more important, but

Table 2. Formation constants used for modeling the Fe^{3+}-citrate system[a]

Species	Constant	Species	Constant
H_3Cit	12.96	$Mn(OH)_4^{2-}$	−47.86
H_2Cit^-	10.06	$MnHCO_3^+$	−4.82
$HCit^{2-}$	5.74	$MnCit^-$	4.18
OH^-	−13.78	$MnHCit^0$	7.86
HCO_3^-	−6.08	$MnCl^+$	0.16
CO_3^{2-}	−16.37	$FeCit^{0b}$	11.52
$CaOH^+$	−13.07	$Fe(OH)Cit^{-b}$	9.88
$CaCO_3^0$	−13.72	$Fe(OH)_2Cit^{2-b}$	2.26
$CaHCO_3^+$	−5.33	$Fe(OH)_2^+$	−2.64
$CaCit^-$	3.38	$Fe(OH)_2^+$	−6.36
$CaHCit^0$	7.96	$Fe(OH)_3^0$	−13.14
CaH_2Cit^+	10.76	$Fe(OH)4^-$	−22.04
$MgOH^+$	−11.66	$Fe2(OH)_2^{4+}$	−3.00
$MgCO_3^0$	−13.52	$FeCl_2^+$	0.84
$MgHCO_3^+$	−5.43	$FeCl_2^+$	1.00
$MgCit^-$	3.38	$FeSO4^+$	2.68
$MgHCit^0$	7.66	$Fe(SO_4)_2^-$	3.64
$MnOH^+$	−10.82	NH_3	−9.3
$Mn(OH)_2^0$	−22.42	HNO_3	−0.78
$Mn(OH)_3^-$	−34.80	HPIPES[c]	6.92

[a] Except where noted, taken from Morel & Hering (1993); constants were adjusted to 0.1 M ionic strength.
[b] Reported at 0.1 M ionic strength by Hamm et al. (1954).
[c] From Joshi-Topé & Francis (1995).

the concentration of $FeCit^0$ is insignificant in this pH range.

To begin the modeling analysis, we fixed the stoichiometry of the reaction for aerobic citrate oxidation coupled to biomass synthesis using energetics principles (McCarty 1972; Rittmann & McCarty 2001; VanBriesen & Rittmann 2000):

$$C_6H_5O_7^{3-} + 0.0725H_2O + 0.642NH_4^+ + 1.287O_2 + 2.358H^+ \rightarrow 0.642C_5H_7O_2N + 2.788H_2CO_3 \quad (16)$$

where $C_6H_5O_7^{3-}$ is citrate, which is the component form used for speciation in CCBATCH. This stoichiometry corresponds to a true yield (Y) of 0.642 mol biomass/mol citrate, or 0.504 gVSS/gThOD, where VSS stands for volatile suspended solids and ThOD stands for theoretical oxygen demand. A maximum electron flow to respiration of 1 e^-eq/gVSS-d (McCarty 1972; Rittmann & McCarty 2001) makes the maximum specific rate of citrate utilization (q_{max}) 1.17 gThOD/gVSS-h at 20 C. Using the Arrhenius equation (E_a = 48.8 kJ/mol) to convert q_{max} to 26 C, the temperature of the experiments, gives q_{max} = 1.75 gThOD/gVSS-h, which also equals 1.37 mol citrate/mol biomass-h. The maximum specific growth rate (μ_{max}) is the product Yq_{max} and equals 0.88 h^{-1} for 26 C. Equation (16) also shows the consumption of 2.358 equivalents of acidic hydrogen (H^+) per mole of citrate consumed, and this feature can result in a pH increase.

Using CCBATCH, we first simulated the experimental results with no Fe^{3+} added to estimate the Monod half-maximum-rate concentration (K_s) for *P. fluorescens* utilizing $HCit^{2-}$ as its only bioavailable substrate (VanBriesen & Rittmann 1999). The curve in the left panel of Figure 1 shows the model results for citrate degraded. The K_s value is 1.3×10^{-6} M, or 0.187 mg ThOD/l. The Monod half-maximum-rate concentration for oxygen (K_a) was set at 6.25×10^{-6} M (0.2 mgO_2/l) (Kinzelbach et al. 1991), a value that exerted no limitation in the experiments. Table 3 summarizes all the parameters used for the kinetics of citrate biodegradation and biomass growth.

We next simulated the results for the experiments having the 1 : 1 mole ratio of Fe^{3+}: citrate added. We used CCBATCH with the biodegradation parameters shown in Table 3, the complexation constants shown on Table 2, and a range of values for the precipitation kinetics. The modeling results for addition of Fe^{3+} at a 1 : 1 mole ratio with citrate (right panel of Figure 1) show that a lumped precipitation-rate coefficient ($k'a$) between 10^9 and 10^{10} h^{-1} gives a good match to the experimental results for citrate degraded. Although the calculated profiles do not correspond precisely for every experimental datum, they capture the overall trend very well: the slow biodegradation of citrate as $Fe(OH)_{3(s)}$ precipitates.

Figure 2 plots model-predicted results for total citrate, biomass, pH, and $Fe(OH)_{3(s)}$ precipitated for $k'a = 10^9$ and 10^{10} h^{-1}. Figure 2 clearly shows that the degradation of citrate occurs together with the precipitation of $Fe(OH)_{3(s)}$. Biomass growth follows $Fe(OH)_{3(s)}$ precipitation. Initially, the system is oversaturated with respect to $Fe(OH)_{3(s)}$, and precipitation begins immediately. The amount of precipitation depends on $k'a$. Precipitation initially results in a small pH drop, since base is removed.

Significant biodegradation begins just after 10 h, and it accelerates around 15 h, when a significant concentration of biomass is present. The biodegradation of citrate removes a triprotic acid (i.e., H_3Cit, as shown in Equation (16)), and this results in a sharp pH increase at the time of accelerating citrate biodegrada-

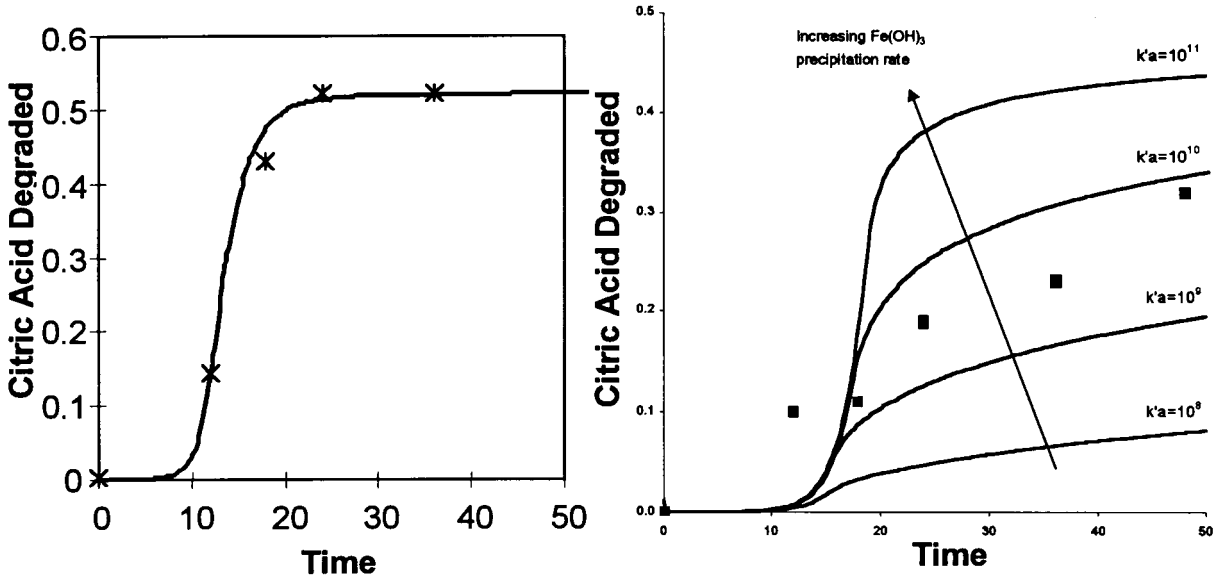

Figure 1. Comparison of model-calculated to experimental results for the biodegradation of citric acid by *P. fluorescens*. The left panel is for no Fe^{3+} addition, while the right panel is for Fe^{3+} addition at a 1 : 1 mole ratio with citrate. All computations are based on $HCit^{2-}$ being the bioavailable species and using the parameters listed in Tables 2 and 3. The $Fe(OH)_{3(s)}$ precipitation rate coefficient (k′a) increases in the order 10^8, 10^9, 10^{10}, and 10^{11} h^{-1} for the right panel.

Table 3. Comparison of the forms of the precipitation rate equations

Parameter	Mole units	Gram units	Source
Y	0.642 mol biomass/mol citrate	0.504 gVSS/g ThOD	Equation (16)
q_{max}	1.37 mol citrate/mol biomass-h	1.5 gThOD/$gVSS^{-1}$	McCarty 1972; Rittmann & McCarty 2001
μ_{max} 0.88 h^{-1}	0.88 h^{-1}	$\mu_{max} = Yq_{max}$	
K_s	1.3×10^{-6} mol $HCit^{2-}$/l	0.187 mg $HCit^{2-}$ ThOD/l	fitting, Figure 1
K_a	6.25×10^{-6} mole O_2/l	2×10^{-1} mgO2/l	Kinzelbach et al., (1991)
b*	0.05 d^{-1}	0.05 d^{-1}	VanBriesen & Rittmann (1999)

* Endogenous decay coefficient.

tion. By 50 h, the model predicts that 35 to 63% of the citrate is biodegraded, while 35 to 63% of the Fe^{3+} is precipitated as $Fe(OH)_{3(s)}$. The pH increases from 6.7 to 7.0 due to the consumption of acidic hydrogen during citrate biodegradation.

Figure 3 presents the model-predicted concentrations for the major iron and citrate species. At the very beginning of the experiment, precipitation of $Fe(OH)_{3(s)}$ consumes Fe^{3+}, which releases citrate, and all the acid/base citrate species increase sharply in concentration. Most significant is the increase in $HCit^{2-}$, the bioavailable form. Coincident is the sharp decrease in pH due to base consumption during $Fe(OH)_{3(s)}$ precipitation (Figure 2). Hence, the bioavailable $HCit^{2-}$ is at its maximum concentration to just beyond 10h, when the biodegradation rate accelerates due to biomass growth.

Biodegradation after about 10 h eventually leads to the loss of all citrate species. The pH increase that occurs in parallel to citrate biodegradation (Figure 2) accentuates the slowdown in biodegradation kinetics, because $HCit^{2-}$ declines more rapidly than other citrate species, particularly Cit^{3-} and $FeOHCit^{-}$. In fact, Cit^{3-} spikes up just as the biodegradation rate begins to slow at 16 to 18 hours.

Figures 2 and 3 compare predicted results for = 10^9 and 10^{10} h^{-1}. The larger k′a value allows more precipitation (Figure 2), although the onset of precipitation occurs at almost the same time. A large biomass inoculum or faster biodegradation kinetics (e.g., a smaller K_s) would allow precipitation to begin

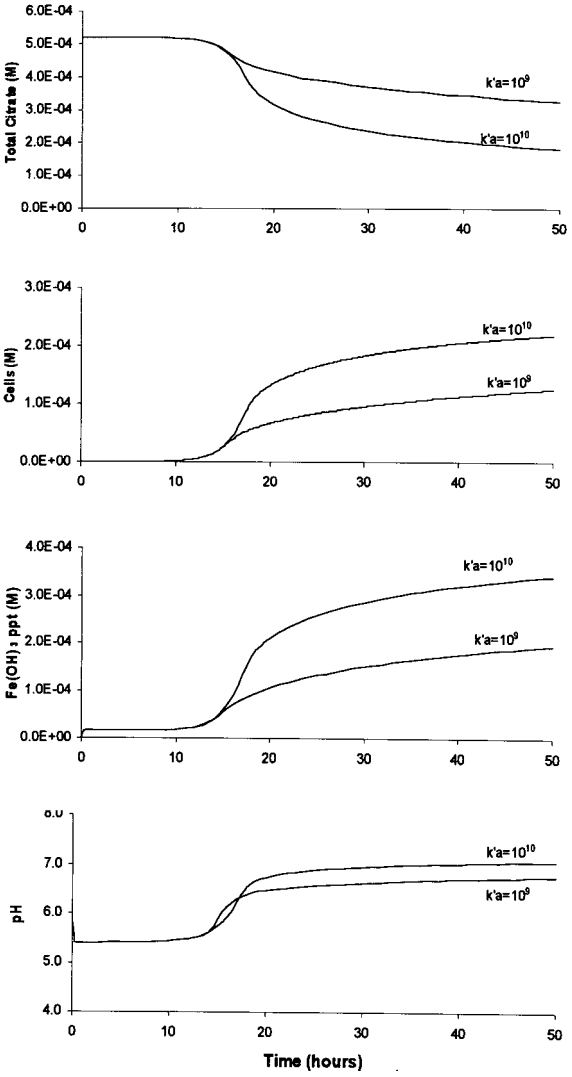

Figure 2. Model-predicted values for total citrate, pH, and $Fe(OH)_{3(s)}$ precipitated for the conditions of the right panel in Figure 1 and with $k'a = 10^9$ and 10^{10} h^{-1}.

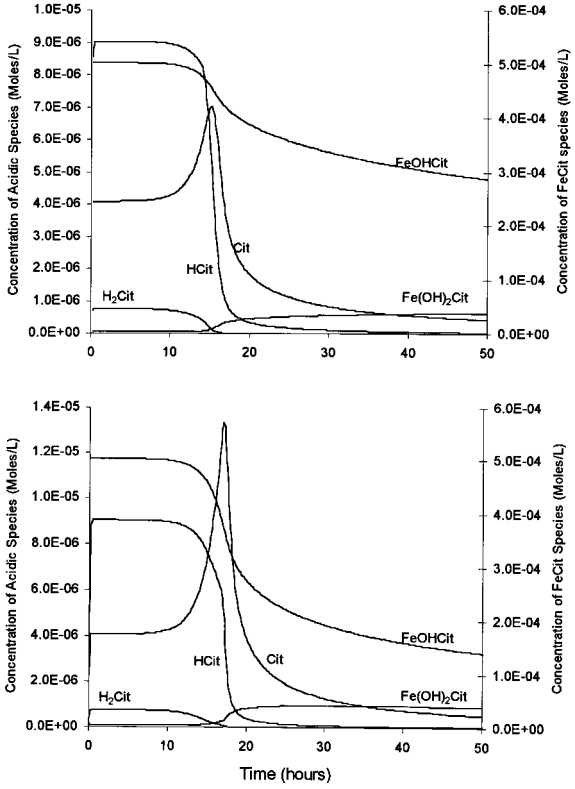

Figure 3. Model-predicted values for major citrate species for the conditions of the right panel in Figure 1 and Figure 2 and with $k'a = 10^9$ (top) and 10^{10} h^{-1} (bottom).

sooner (data not shown), but $k'a$ controls the rate of precipitation and the long-term biodegradation of citrate, growth of cells, and pH increase. The patterns for changes in speciation (Figure 3) are similar for both $k'a$ values, but the larger $k'a$ allows more dramatic change in major species, $FeOHCit^-$ and Cit^{3-}.

Conclusions

Because precipitation and dissolution interact with microorganisms and their metabolic reactions, we expanded the biogeochemical model CCBATCH to include a precipitation/dissolution sub-model. We took advantage of the fact that different reaction mechanisms yield a common kinetic expression, Equation (15). This expression explicitly incorporates reaction or mass-transfer kinetics, the difference from thermodynamic equilibrium, and the aqueous concentration of the rate limiting metal or ligand.

The precipitation/dissolution sub-model can be used in equilibrium or kinetic modes. When the precipitation/dissolution sub-model predicts kinetically controlled precipitation or dissolution, it also includes an equilibrium check that prevents a predicted rate from being too fast and "overshooting" equilibrium.

The features of the expanded CCBATCH are illustrated with a example in which *P. fluorescens* biodegrades citrate in the presence of an initial 1 : 1 mole ratio of Fe^{3+}, even though Fe^{3+}-citrate complexes are strong and unavailable for biodegradation. The expanded CCBATCH demonstrates that the solution is super-saturated with respect to $Fe(OH)_{3(s)}$, which begins precipitating. Precipitation releases citrate and reduces the pH, both of which increase the concentra-

tion of bioavailable $HCit^{2-}$ and allow biodegradation of citrate. Sustained citrate biodegradation consumes the acidic hydrogen, which increases the pH and gradually slows biodegradation, particularly because the bioavailable $HCit^{2-}$ species declines very rapidly due to the combined effects of a decrease in the total citrate and an increase in the pH.

Acknowledgements

This research was funded in part by a grant from the United States Department of Energy. The continued support of Dr. Frank Wobber is gratefully acknowledged. The authors also acknowledge Drs. A. J. Francis and G. Joshi-Topé for fruitful discussions.

References

Bae W & Rittmann BE (1996) A structured model of dual-limitation kinetics. Biotechnol. Bioeng. 49: 683–689

Banaszak JE (1999) Coupling microbial and mineral-phase reactions. PhD dissertation, Dept. Civil Eng., Northwestern Univ., Evanston, Illinois

Bethke CM (1992) The geochemists' workbench, a users' guide to Rxn, act 2, tact, react. and Gtp[lot]. Dept. of Geology, University of Illinois at Urbana-Champaign, Urbana, Illinois.

Borse GJ (1991) FORTRAN 77 and numerical methods for engineers, 2nd edn, PWS-KENT Publishing Co., Boston.

Brady PV & House WA (1996) Surface-controlled dissolution and growth of minerals. In: PV Brady (Ed), Physics and Chemistry of Mineral Surfaces (pp. 225–306). CRC Press, Boca Raton, Florida

Brady PV & Zachara JM (1996) Geochemical applications of mineral surface science. In: PV Brady (Ed), Physics and Chemistry of Mineral Surfaces, (pp. 307-356). CRC Press, Boca Raton, Florida

Flint RA (1963) Fundamentals of Metal Casting, Addison-Wesley Co., Reading, Massachusetts

Hamm RE, Shull CMJ & Grant DM (1954) Citrate complexes with iron (II) and iron (III). J. Amer. Chem. Soc. 76: 2111–2114

Jordan, AD & Rammensee W (1996) Dissolution rates and activation energy for dissolution of brucite (001): a new method based on the microtopography of crystal surfaces. Geochimica et Cosmochimica Acta 60: 5055–5062

Joshi-Topé G & Francis AJ (1995) Mechanisms of biodegradation of metal-citrate complexes by *Pseudomonas fluorescens*. J. Bacteriology 177: 1989–1993

Kinzelbach W, Schäfer W & Herzer J (1991) Numerical modeling of natural and enhanced denitrification processes in aquifers. Water Resource Res. 27: 1123–1135

Lasaga AC (1995) Fundamental approaches in describing mineral dissolution and precipitation rates. In: AF White & SL Brantley (Eds), Chemical Weathering Rates of Silicate Minerals Cycles. Mineralogical Soc. Amer. 31: 21–86

Lasaga AC, Soler, JM, Ganor, J, Burch, TE & Nagy KL (1994) Chemical weathering rate laws and global geochemical cycles. Geochemica et Cosmochimica Acta 58: 2361–2386

Lichtner PC (1985) Continuum model for simultaneous chemical reactions and mass transport in hydrothermal systems. Geochemica et Cosmochimica Acta 49: 779–800

Lichtner PC (1996) Continuum formulation of multicomponent-multiphase reactive transport. In: PC Lichtner, CI Steefel & EH Oelkers (Eds), Rev. in Mineralogy, Vol. 34: Reactive Transport in Porous Media. Mineralogical Soc. Amer

Lovley DR (1991) Dissimilatory Fe(III) and Mn(IV) reduction. Microbial. Rev. 55: 259–287

Madigan MT, Martinko JM & Parker J (2000) Brock Biology of Microorganisms, 9th ed., Prentice-Hall, Inc., Upper Saddle Ridge, New Jersey

McCarty PL (1972) Energetics of organic matter degradation. In: R. Mitchell (Ed), Water Pollution Microbiology (pp. 98–118). John Wiley & Sons, Inc., New York

Morel FMM & Hering JG (1993) Principles and Applications of Aquatic Chemistry, John Wiley & Sons, Inc., New York

Morel FMM & Morgan J (1972) A numerical method for computing equilibria in aqueous chemical systems. Environ. Sci. Technol. 6: 58–67

Myers CR & Myers JM (1993) Ferric reductase is associated with the membranes of anaerobically grown *Shewanella putrafaciens*. FEMS Microb. Letters 108: 127–131

Paquette J & Reeder RJ (1995) Relationship between surface structure, growth mechanism and trace element incorporation in calcite. Geochemica et Cosmochimica Acta 59: 735–749

Press WH, Teukolsky SA, Vettering WT & Flannery BP (1992) Numerical Recipes in FORTRAN: The Art of Scientific Computing. Cambridge University Press, New York

Rittmann BE & McCarty PL (2001) Environmental Biotechnology: Principles and Applications. McGraw-Hill Book Co., New York

Rittmann BE & VanBriesen JM (1996) Microbiological processes in reactive transport modeling. In: PC Lichtner, CI Steefel & EH Oelkers (Eds), Reactive Transport in Porous Media, Vol. 34 (pp. 311–334). Mineralogical Soc. Amer., Washington, DC

Stumm W & Morgan JJ (1996) Aquatic Chemistry, 3rd edn John Wiley & Sons, Inc., New York

VanBriesen JM & Rittmann BE (1999) Modeling speciation effects on biodegradation in mixed metal/chelate systems. Biodegradation 10: 315–330

VanBriesen JM & Rittmann BE (2000) Mathematical description of microbiological reactions involving intermediates. Biotechnol. Bioengr. 67: 18–52.